

A Theoretical Analysis of the Spatial Multi Channel Compressed Sensing Model

Tobias Schnier, Carsten Bockelmann, Armin Dekorsy
Department of Communications Engineering
University of Bremen, Germany
Email: {schnier,bockelmann,dekorsy}@ant.uni-bremen.de

Abstract—The Compressed Sensing (CS) framework is heavily utilized to reduce data rate in hardware restricted scenarios by exploiting the intrinsic sparsity of the transmitted data. Considering multiple sensors at the same time, one variation of the Multi Channel (MC) framework takes several measurements at one time instant and then uses CS in the spatial domain to compress the data. This paper provides a theoretical analysis of the proposed system by computing the coherence and the Restricted Isometry Constant (RIC) of the corresponding MC sensing matrix. Additionally, we provide simulation results to further show the applicability and advantages of this system.

Index Terms—CS, Multi Channel, Analysis, Joint sparsity, Coherence, RIP

I. INTRODUCTION

A. Motivation

The problem of reducing the data rate in data accumulation applications is as important as it is prominent. A common approach is the *Compressed Sensing* (CS, [1]) framework which uses a sparsity assumption to compress signals far below the Nyquist rate. One of the applications of interest is the Magnetic Resonance Imaging (MRI) system that is shown to make good use of the CS setup as typical MRI images are sparse in the Wavelet basis [2]. By implementing CS, the data rate reduction directly transfers to a reduced time for the patient inside the MRI, which is still one of the key problems of state of the art machines. Another important application are wireless devices that can record in vivo neural signals. Due to the fact that the required Nyquist sampling rate are hard to reach in the given harsh hardware requirements, CS approaches can be utilized to reduce the data rate further. Sadly, while still achieving promising results for both mentioned applications, the rates are far from sufficient for many purposes, so for next generation devices we need to take into account every possibility of reduction.

To this end, a *Multi Channel* (MC) model was proposed [3], which considers several signals at once. With possibly some joint sparsity assumptions [4], the combined reconstruction needs less samples than reconstructing each signal individually. For MRI, this idea has gained traction in research (e.g. [5],[6]) due to the fact that the MRI acquisition devices have several sensors that are highly correlated to each other. Furthermore, Neuro applications directly profit from this idea, as already state of the art devices use sensor arrays [7]. The resulting measurement signals are often correlated and are

well matched to the joint sparsity approach, so they can easily utilize the joint reconstruction idea.

Unfortunately, for optimal hardware implementability and thus real applications, the standard MC model is insufficient. As typically the sparsity assumption is over time, we need to consider the behavior of hardware over time. For implementation of standard CS systems, the measurements are stored in capacitors to be read at fixed time intervals. If charge is lost due to natural discharge processes, the values are inaccurate and thus lead to reconstruction errors. To counter this, amplifiers are used, but they come with high area and energy demands, which do not fit the hardware constraints in the Neuro setting. Luckily, a variation of the MC model can circumvent the problem of charge loss. In contrast to the standard model, we consider acquiring the CS measurements not as weighted samples over a time frame for each sensor individually but instead over a *weighted sum over all sensors for each time slot*. Thus, we coin the model *spatial Multi Channel*. This way, no capacities between time slots are needed, but a new problem arises. In contrast to the temporal sparsity assumption that is still valid for every time frame, spatial sparsity is not given. In fact, if there is a high correlation between the sensors, the sparsity assumption in sensor direction is violated with high probability. Still, we will show that the MC system should be considered by giving a firm mathematical basis for this system.

One of the standard analysis tools in CS is the *Restricted Isometry Property* (RIP,[1]), which can be used to assess the quality of the used sensing matrix to provide reconstruction guarantees. The importance of the RIP is shown by the many variants and discussions in the CS community, e.g. [8]. As the RIP of a given sensing matrix is NP hard to compute [9] a firm mathematical analysis of given settings is the only way to evaluate the quality of a proposed system. Another important property is the *coherence* [10] of the sensing matrix which is a measure of the similarity of the different dictionary atoms. Due to the fact that the coherence is directly linked to the required CS measurements for optimal reconstruction, a low coherence system is of high interest for strict hardware constraints and thus data rate limited systems. Especially when using the very prominent Orthogonal Matching Pursuit (OMP) algorithm [7], the coherence plays a key role in the reconstruction.

B. Main Contribution

In this paper, we analyze the spatial Multi Channel model. For this, we establish and prove the exact value of the coherence and show theoretical boundaries for the RIP constant of the MC model. Additionally, we provide simulation results to further justify the mathematical theory and show comparisons to the standard CS system. In result, we show that the proposed system is not only highly implementable with low energy and area costs but also has comparable RIP constants and an even better coherence than the standard CS system.

II. THE MULTI CHANNEL MODEL

A. Mathematical Preliminaries

In standard CS, a sparsely representable vector $\mathbf{x} \in \mathbb{R}^N$ is measured with help of the measurement matrix $\Phi \in \mathbb{R}^{m \times N}$ to get the measurements \mathbf{y} . Additionally, the vector \mathbf{x} can be represented by its dictionary $\Psi \in \mathbb{R}^{N \times N}$ with the form $\mathbf{x} = \Psi \mathbf{c} \in \mathbb{R}^N$ and the **sparse** vector $\mathbf{c} \in \mathbb{R}^N$. The resulting measurements $\mathbf{y} = \Phi \mathbf{x} = \Phi \Psi \mathbf{c} \in \mathbb{R}^m$ can now be used to define the overall matrix $\mathbf{A} = \Phi \Psi \in \mathbb{R}^{m \times N}$ that directly transfers from the sparse vector \mathbf{c} to the CS measurements. If L data vectors $\mathbf{x}_i = \Psi \mathbf{c}_i$, $i = 1, \dots, L$ are considered, the whole CS system can be cast in the form

$$\mathbf{A}_{CS} = \begin{pmatrix} \Phi & 0 \\ & \ddots \\ 0 & \Phi \end{pmatrix} \begin{pmatrix} \Psi & 0 \\ & \ddots \\ 0 & \Psi \end{pmatrix} \quad (1)$$

with possibly different sensing matrices $\Phi^{[i]}$ and the overall matrix $\mathbf{A}_{CS} \in \mathbb{R}^{mL \times NL}$ which easily decomposes into smaller problems. Still, this formal setting is useful if there are joint sparsity assumptions [4] that link the problems.

In the **spatial** Multi Channel scenario, the measurements are **not taken individually at each of the L sensors**, but the sensing step is done over **all** sensors for each individual element of \mathbf{x} , so now the sensing matrix has the dimensions $\Phi \in \mathbb{R}^{m \times L}$. It is important to note, that the dictionary representation (and thus the sparsity assumption) is still in the standard CS sense, so the complete problem can not be divided into smaller parts anymore. Instead the whole system must be reconstructed with one overall measurement matrix that we will further analyze in this paper. Formally, the spatial MC system can be cast in the form of

$$\begin{pmatrix} \mathbf{y}_1 \\ \vdots \\ \mathbf{y}_N \end{pmatrix} = \begin{pmatrix} \Phi & 0 \\ & \ddots \\ 0 & \Phi \end{pmatrix} \begin{pmatrix} x_{1,1} \\ \vdots \\ x_{1,L} \\ \vdots \\ x_{N,1} \\ \vdots \\ x_{N,L} \end{pmatrix} \quad (2)$$

This system can be reordered by permutating the rows of the whole \mathbf{x} -vector and respectively the columns of the Φ matrix in a way that the temporal parts \mathbf{x}_i emerge again. With the

definition of $\Psi_i \in \mathbb{R}^{N \times 1}$ as the i -th column of Ψ , the system takes the form

$$\begin{pmatrix} \mathbf{y}_1 \\ \vdots \\ \mathbf{y}_N \end{pmatrix} = \begin{pmatrix} \Phi_1 & 0 & \cdots & \Phi_L & 0 \\ & \ddots & & & \ddots \\ 0 & & \Phi_1 & \cdots & 0 & \Phi_L \end{pmatrix} \begin{pmatrix} x_{1,1} \\ \vdots \\ x_{N,1} \\ \vdots \\ x_{1,L} \\ \vdots \\ x_{N,L} \end{pmatrix} \\ = \begin{pmatrix} \Phi_1 & 0 & \cdots & \Phi_L & 0 \\ & \ddots & & & \ddots \\ 0 & & \Phi_1 & \cdots & 0 & \Phi_L \end{pmatrix} \begin{pmatrix} \mathbf{x}_1 \\ \vdots \\ \mathbf{x}_L \end{pmatrix}$$

with

$$\begin{pmatrix} \mathbf{x}_1 \\ \vdots \\ \mathbf{x}_L \end{pmatrix} = \begin{pmatrix} \Psi & 0 \\ & \ddots \\ 0 & \Psi \end{pmatrix} \begin{pmatrix} \mathbf{c}_1 \\ \vdots \\ \mathbf{c}_L \end{pmatrix} \quad (3)$$

In this form, the attributes of \mathbf{x}_i (i.e. $\mathbf{x}_i = \Psi \mathbf{c}_i$) can be used to further refine the system of equations. If we compare

$$\mathbf{A}_{CS} = \begin{pmatrix} \Phi & 0 \\ & \ddots \\ 0 & \Phi \end{pmatrix} \begin{pmatrix} \Psi & 0 \\ & \ddots \\ 0 & \Psi \end{pmatrix} \quad (4)$$

$$\mathbf{A}_{MC} = \begin{pmatrix} \Phi_1 & 0 & \cdots & \Phi_L & 0 \\ & \ddots & & & \ddots \\ 0 & & \Phi_1 & \cdots & 0 & \Phi_L \end{pmatrix} \begin{pmatrix} \Psi & 0 \\ & \ddots \\ 0 & \Psi \end{pmatrix} \quad (5)$$

it is easy to see that the multiplication of the Φ and the Ψ matrices is a *diagonal* matrix in the CS case and a *dense* matrix in the MC case. To really asses the quality of the MC scheme, we need to further analyse and compare these two sensing matrices. Of special interest here is the coherence μ and the RIP constants δ_k of the two matrices. To better analyze the MC sensing matrix \mathbf{A}_{MC} , we first evaluate the inherent product by noticing that the block $\mathbf{A}_{MC,ij}$ of size $m \times N$ can be written as the rank 1 matrix

$$\mathbf{A}_{MC,ij} = \Phi_i \Psi^j \in \mathbb{R}^{m \times N} \quad (6)$$

with Φ_i being the i -th column of Φ and Ψ^j being the j -th row of Ψ . Using (7), we can rewrite the MC matrix as

$$\mathbf{A}_{MC} = \begin{pmatrix} \Phi_1 \Psi^1 & \cdots & \Phi_L \Psi^1 \\ \vdots & \ddots & \vdots \\ \Phi_1 \Psi^N & \cdots & \Phi_L \Psi^N \end{pmatrix} \in \mathbb{R}^{mN \times LN} \quad (7)$$

In contrast to that, the block structure of \mathbf{A}_{CS} is directly visible as the product of two block diagonal matrices

$$\mathbf{A}_{CS,ij} = \begin{cases} \Phi \Psi & \text{if } i = j \\ 0 & \text{if } i \neq j \end{cases} \in \mathbb{R}^{mL \times NL} \quad (8)$$

B. Coherence

In this section, we will now analyze the coherence of the MC matrix. Formally, the coherence is defined as

$$\mu(\mathbf{A}) := \max_{i \neq j} \frac{(\mathbf{A}^T \mathbf{A})_{ij}}{\|\mathbf{A}_i\| \|\mathbf{A}_j\|}. \quad (9)$$

The main result of the result is shown in the following theorem.

Theorem 1. Let $\Phi \in \mathbb{R}^{m \times L}$, $\Psi \in \mathbb{R}^{N \times N}$ and define \mathbf{A}_{MC} as in (8). Then

$$\mu(\mathbf{A}_{MC}) = \max(\mu(\Phi), \mu(\Psi)) \quad (10)$$

In other words, to get a low coherence MC matrix, both sensing and dictionary matrix need to have low coherence themselves. Remarkably, the product $\Phi\Psi$ does not matter in the Multi Channel case.

Proof. To compute the coherence, we first analyze the $N \times N$ blocks of $\mathbf{A}^T \mathbf{A}$ as

$$(\mathbf{A}^T \mathbf{A})_{ij} = ((\Phi_i \Psi^1)^T \dots (\Phi_i \Psi^N)^T) \begin{pmatrix} \Phi_j \Psi^1 \\ \vdots \\ \Phi_j \Psi^N \end{pmatrix} \quad (11)$$

$$\stackrel{(a)}{=} \Phi_i^T \Phi_j \sum_{l=1}^N (\Psi^l)^T \Psi^l \quad (12)$$

$$\stackrel{(b)}{=} \Phi_i^T \Phi_j \Psi^T \Psi \quad (13)$$

where (a) uses the fact that $\Phi_i^T \Phi_j$ is a constant scalar that is independent of the sum index l and (b) is true because of the rank 1 representation of $\Psi^T \Psi$ as the above sum. In other words, the matrix $\mathbf{A}^T \mathbf{A}$ can be represented in the form

$$\mathbf{A}^T \mathbf{A} = \begin{pmatrix} \Phi_1^T \Phi_1 \Psi^T \Psi & \dots & \Phi_1^T \Phi_N \Psi^T \Psi \\ \vdots & \ddots & \vdots \\ \Phi_N^T \Phi_1 \Psi^T \Psi & \dots & \Phi_N^T \Phi_N \Psi^T \Psi \end{pmatrix} \quad (14)$$

Additionally, we need to compute the norms $\|\mathbf{A}_i\|$ with block index k, l computed as

$$i = kN + l \quad (15)$$

to find the corresponding block and inner column. With these indices, the norm can be computed as

$$\|\mathbf{A}_i\|^2 = \sum_{j=1}^N \|\Phi_k \Psi_{l,j}\|^2 \quad (16)$$

$$= \|\Phi_k\|^2 \sum_{j=1}^N \|\Psi_{l,j}\|^2 = \|\Phi_k\|^2 \|\Psi_k\|^2 \quad (17)$$

It follows that

$$\|\mathbf{A}_i\| = \|\Phi_k\| \|\Psi_k\| \quad (18)$$

Altogether, we can now compute the coherence

$$\mu(\mathbf{A}) := \max_{i \neq j} \frac{(\mathbf{A}^T \mathbf{A})_{ij}}{\|\mathbf{A}_i\| \|\mathbf{A}_j\|} \quad (19)$$

with row block indices k_i, l_i and column block indices k_j, l_j computed as

$$i = k_i N + l_i \quad j = k_j N + l_j \quad (20)$$

to be

$$\mu(\mathbf{A}) = \max_{i \neq j} \frac{\Phi_{k_i}^T \Phi_{k_j} \Psi_{l_i}^T \Psi_{l_j}}{\|\Phi_{k_i}\| \|\Psi_{l_i}\| \|\Phi_{k_j}\| \|\Psi_{l_j}\|} \quad (21)$$

or rearranged as

$$\mu(\mathbf{A}) = \max_{i \neq j} \left(\frac{\Phi_{k_i}^T \Phi_{k_j}}{\|\Phi_{k_i}\| \|\Phi_{k_j}\|} \cdot \frac{\Psi_{l_i}^T \Psi_{l_j}}{\|\Psi_{l_i}\| \|\Psi_{l_j}\|} \right). \quad (22)$$

Finding the maximum for $i \neq j$ leads to either $k_i \neq k_j$ or $l_i \neq l_j$ but not both due to Cauchy Schwartz (each fraction is less than 1 for unequal indices). If $k_i = k_j$ the formula collapses to

$$\mu(\mathbf{A})_{k_i=k_j} = \max_{i \neq j} \left(\frac{\Psi_{l_i}^T \Psi_{l_j}}{\|\Psi_{l_i}\| \|\Psi_{l_j}\|} \right) = \mu(\Psi). \quad (23)$$

For $l_i = l_j$ with analogue reasoning the equation

$$\mu(\mathbf{A})_{l_i=l_j} = \max_{i \neq j} \left(\frac{\Phi_{k_i}^T \Phi_{k_j}}{\|\Phi_{k_i}\| \|\Phi_{k_j}\|} \right) = \mu(\Phi) \quad (24)$$

arises. Altogether, the maximum of both values is the true coherence so

$$\mu(\mathbf{A}_{MC}) = \max(\mu(\Psi), \mu(\Phi)) \quad (25)$$

describes the desired result. \square

C. Restricted Isometry Property

In this section, we will analyze the restricted isometry property (RIP) of the MC matrix $\mathbf{A} := \mathbf{A}_{MC}$ of equation (8). Formally, the RIP regarding sparsity k is defined as the smallest number δ_k in $(0, 1)$, such that

$$(1 - \delta_k) \|\mathbf{c}\|_2^2 \leq \|\mathbf{A}\mathbf{c}\|_2^2 \leq (1 + \delta_k) \|\mathbf{c}\|_2^2 \quad (26)$$

for all k sparse vectors \mathbf{c} at each of the L sensors or in other words for a total sparsity of kL . The main result of the section is shown in the following theorem.

Theorem 2. Let $\Phi \in \mathbb{R}^{m \times L}$, $\Psi \in \mathbb{R}^{N \times N}$ and define \mathbf{A}_{MC} as in (8). Then

$$\delta_k(\mathbf{A}_{MC}) = 1 \quad (27)$$

holds for all $k > \frac{mL}{N}$, thus the reconstruction is guaranteed to fail.

Proof. By rewriting the first inequality of the RIP we get

$$1 - \delta_k \leq \frac{\|\mathbf{A}\mathbf{c}\|_2^2}{\|\mathbf{c}\|_2^2} \quad \forall \mathbf{c} \in \mathbb{R}^{NL}, \mathbf{c} \text{ } kL\text{-sparse} \quad (28)$$

or in other words

$$1 - \delta_k = \min_{\mathbf{c} \text{ } k\text{-sparse}} \frac{\|\mathbf{A}\mathbf{c}\|_2^2}{\|\mathbf{c}\|_2^2}. \quad (29)$$

To analyze the RIP, we will first start with structured \mathbf{c} of the form

$$\mathbf{c} = (\mathbf{c}_1^T, \dots, \mathbf{c}_N^T)^T \quad (30)$$

with

$$\mathbf{c}_i = \alpha_i \mathbf{w} \quad (31)$$

with scalar α_i and one vector $\mathbf{w} \in \mathbb{R}^L$ for all parts of \mathbf{c} . By inferring this structure, we lose the generality of the RIP constant, so we can only compute an upper boundary

$$1 - \delta_k = \min_{\mathbf{c} \text{ } k\text{-sparse}} \frac{\|\mathbf{A}\mathbf{c}\|_2^2}{\|\mathbf{c}\|_2^2} \leq \min_{\mathbf{c}_i = \alpha_i \mathbf{w}} \frac{\|\mathbf{A}\mathbf{c}\|_2^2}{\|\mathbf{c}\|_2^2} \quad (32)$$

on the RIP constant δ_k . For clarification, additionally define

$$\boldsymbol{\alpha} := (\alpha_1, \dots, \alpha_L)^T \quad \mathbf{y} := (\mathbf{y}_1^T, \dots, \mathbf{y}_N^T)^T \quad (33)$$

and $\mathbf{y} = \mathbf{A}\mathbf{c}$. With this structured vector \mathbf{c} , we can now compute the vectors $\mathbf{y}_j = \mathbf{A}^j \mathbf{c}$ with \mathbf{A}^j as the j -th row of the block matrices as

$$\begin{aligned} \mathbf{y}_j &= \mathbf{A}^j \mathbf{c} \stackrel{(a)}{=} \begin{pmatrix} \Phi_1 \Psi^j & \dots & \Phi_L \Psi^j \end{pmatrix} \begin{pmatrix} \mathbf{c}_1 \\ \vdots \\ \mathbf{c}_L \end{pmatrix} \\ &\stackrel{(b)}{=} \sum_{i=1}^L \Phi_i \Psi^j \alpha_i \mathbf{w} \stackrel{(c)}{=} \Phi \boldsymbol{\alpha} \Psi^j \mathbf{w} \end{aligned}$$

where (a) uses the definition of \mathbf{A} and \mathbf{c} , (b) uses the structure of \mathbf{c} in (32) and (c) is possible, because $\Psi^j \mathbf{w}$ are independent of the summation index. With this, we can now compute the norm $\|\mathbf{A}\mathbf{c}\|$ as needed for the RIP property:

$$\|\mathbf{A}\mathbf{c}\| = \|\mathbf{y}\| \stackrel{(a)}{=} \sqrt{\sum_{j=1}^N \underbrace{\|\Phi \boldsymbol{\alpha} \Psi^j \mathbf{w}\|}_{\text{scalar}}^2} \stackrel{(b)}{=} \|\Phi \boldsymbol{\alpha}\| \|\Psi \mathbf{w}\| \quad (34)$$

Here, (a) is the insertion of the last result and (b) uses the definition of the norm. Additionally, we need to compute $\|\mathbf{c}\|$ as

$$\begin{aligned} \|\mathbf{c}\| &\stackrel{(a)}{=} \sqrt{\sum_{i=1}^N \|\mathbf{c}_i\|^2} \stackrel{(b)}{=} \sqrt{\sum_{i=1}^N \|\alpha_i \mathbf{w}\|^2} \\ &\stackrel{(c)}{=} \|\mathbf{w}\| \sqrt{\sum_{i=1}^N \|\alpha_i\|^2} \stackrel{(d)}{=} \|\mathbf{w}\| \|\boldsymbol{\alpha}\| \end{aligned}$$

with the exact same steps as above to get the result

$$\|\mathbf{c}\| = \|\mathbf{w}\| \|\boldsymbol{\alpha}\|. \quad (35)$$

With help of the equations (35) and (36) above, we can further refine the upper bound of the RIP constant in equation (33) to

$$\frac{\|\mathbf{A}\mathbf{c}\|_2^2}{\|\mathbf{c}\|_2^2} = \frac{\|\Phi \boldsymbol{\alpha}\|_2^2}{\|\boldsymbol{\alpha}\|_2^2} \frac{\|\Psi \mathbf{w}\|_2^2}{\|\mathbf{w}\|_2^2}. \quad (36)$$

Due to $\Phi \in \mathbb{R}^{m \times N}$ and $m < N$, the null space of Φ always exists. Choosing $\boldsymbol{\alpha}$ as any vector in the null space cancels out the equation to zero. As the formula is an **upper** boundary for $1 - \delta_k$ and $\delta_k \in [0, 1]$, δ_k has to be equal to 1. Due to the fact, that the sparsity of \mathbf{c} is the sparsity of \mathbf{w} ($\boldsymbol{\alpha}$ is dense), this reasoning holds for all k that fulfill $kN > mL$. \square

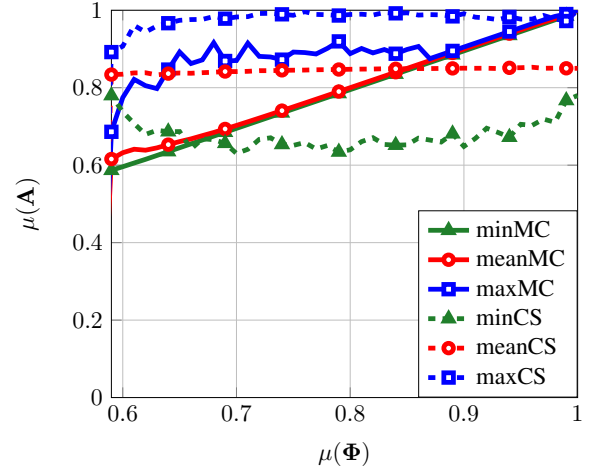


Fig. 1. Simulated coherence of the MC and CS matrix \mathbf{A} plotted against the coherence of the sensing matrix Φ . For each case, the minimum, mean and maximum values are shown.

In conclusion, again the RIP constants can be computed by the division into a sensing and a dictionary part, while the standard CS approach operates on the the product of both. As in the MC case the division affects the RIP constants in a destructive way, the overall constants will be worse in comparison and even tend to zero for high enough sparsities k .

III. NUMERICAL SIMULATIONS

This section provides numerical validations for the theoretical results above. In Fig. 1, the coherence of the multi-channel approach and the standard CS setting is plotted against the coherence of the sensing matrix Φ after 10^6 trials. Both matrices $\Phi \in \mathbb{R}^{10 \times 20}$ and $\Psi \in \mathbb{R}^{20 \times 20}$ are random Gaussian matrices ($\mu = 0, \sigma = 1$). The coherence of the resulting matrices $\mathbf{A}_{MC}, \mathbf{A}_{CS} \in \mathbb{R}^{200 \times 400}$ is plotted with solid line for the MC case and the dashed line for the standard CS setting. The lines show the minimum (green, triangle), mean (red, circle) and maximum (blue, square) results for the corresponding matrices. It is directly visible that in the MC case the mean value lies very close to the minimal value, which coincides with $\mu(\Phi)$. There are some outliers which lie above the mean, but the number of outliers is so low that even after 10^6 trials, there is still a high variance left. For higher coherences (around $\mu(\Phi) = 0.87$), all three lines nearly match which underlines the statement $\mu(\mathbf{A}_{MC}) = \max(\mu(\Phi), \mu(\Psi))$. In contrast to that, the standard CS case (dashed lines) has a constant mean value, regardless of the coherence of Φ . This is due to the fact that only the product $\Phi \Psi$ defines the coherence and a separation is impossible. Additionally, the fluctuations around the mean are a lot higher with maximum values of nearly one and lower values (down to 0.6) for the minimum. All in all, the MC case shows a better performance as the mean values for randomly chosen dictionaries can be influenced by a large margin with the choice of a low coherent sensing matrix while the CS case cannot be influenced.

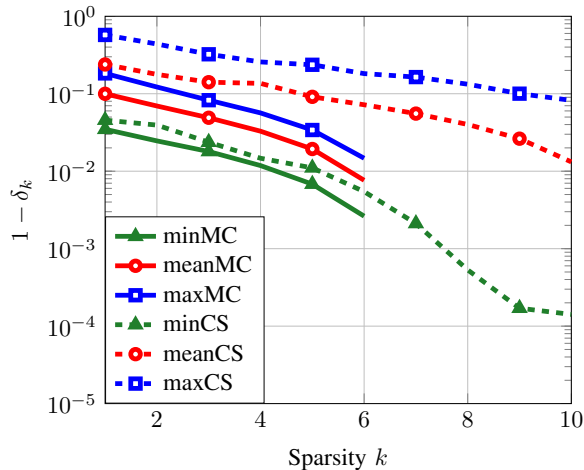


Fig. 2. Numerically computed RIP constants of the MC and CS case plotted against the corresponding sparsities k . For each case, the minimum, mean and maximum values are shown.

Fig. 2 shows the logarithmic plot of the complementary RIP constants of randomly chosen dictionary and sensing matrices for $m = 10$, $N = 30$ and $L = 20$ plotted against the sparsity k of \mathbf{w} for the sparsity pattern $\mathbf{c}_i = \alpha_i \mathbf{w}$. In result, the matrices have the dimension $\mathbf{A}_{MC}, \mathbf{A}_{CS} \in \mathbb{R}^{200 \times 600}$ with the overall resulting sparsity of kL . Here, the NP hard problem of computing the RIP constants is done by exhaustive search over all possible sparse variations. Again, due to the random choice of Ψ in each iteration, there are variations in the RIP constants, so the maximum values (blue plot), the mean values (red plot) and the minimum values (green plot) are shown for each sparsity. It can be directly seen that in the MC case the results are overall worse and have a smaller variation in comparison to the standard CS setting. It is notable, that even the maximum value of the MC case cannot achieve the mean RIP constants of the standard setting. At a sparsity of $k = 7$ the RIP constants reach one due to $kN > mL$ as shown in section II-C, so the resulting complementary logarithmic plot cannot be shown anymore. In contrast to that, for the standard CS case a more gradual plot emerges with RIP values slowly approaching and finally reaching zero at $k = 11$ ($k > m$). This setting is chosen specifically to show the downsides of MC as the fraction L/N is low. Luckily, in higher scale problems with a higher number of sensors this problem diminishes.

Fig. 3 shows the percentage of recovered indices of the OMP algorithm for the two systems in comparison. Here it can be seen that first the MC case is superior due to the higher coherence and still good RIP constants. For higher sparsities this effect reverses because now the RIP constants dominate the recovery, so the standard CS case takes the lead. All in all, these effects are only small, so they both have comparable recovery properties.

IV. CONCLUSION

In this paper, we have computed the coherence and RIP constants in the Multi Channel setting. We showed, that for

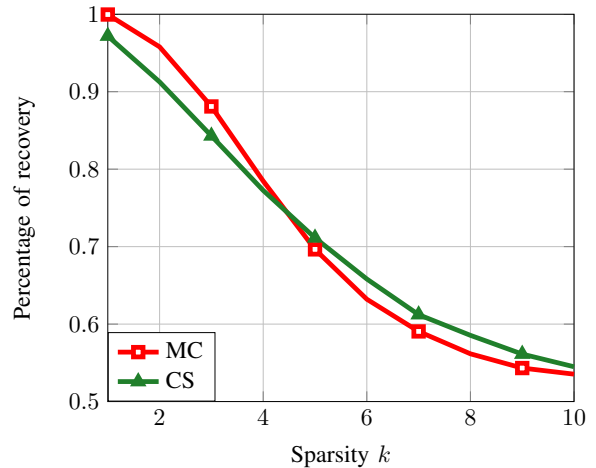


Fig. 3. Percentage of recovered indices for the OMP algorithm in the MC and CS case plotted against the corresponding sparsities k .

good sensing matrices, the MC setting will have a better coherence but worse Restricted Isometry Constants than using the same sensing matrix in the standard setting. Additionally, we provided numerical simulations to justify the theoretical insights. We showed that the Multi Channel setting is a valuable alternative to the standard CS scheme that is able to reduce the needed hardware by a large margin.

ACKNOWLEDGMENT

This work was funded by the German Research Foundation (DFG) under grant DE 759/5-1.

REFERENCES

- [1] D. L. Donoho, "Compressed sensing," *Information Theory, IEEE Transactions on*, vol. 52, no. 4, pp. 1289–1306, 2006.
- [2] M. Lustig, D. Donoho, and J. M. Pauly, "Sparse mri: The application of compressed sensing for rapid mr imaging," *Magnetic resonance in medicine*, vol. 58, no. 6, pp. 1182–1195, 2007.
- [3] J. Slavinsky, J. N. Laska, M. A. Davenport, and R. G. Barniuk, Eds., *The compressive multiplexer for multi-channel compressive sensing*. IEEE, 2011.
- [4] M. Duarte, S. Sarvotham, M. Wakin, D. Baron, and R. Baraniuk, Eds., *Joint sparsity models for distributed compressed sensing*, 2005.
- [5] C.-H. Chang and J. Ji, "Compressed sensing mri with multichannel data using multicore processors," *Magnetic resonance in medicine*, vol. 64, no. 4, pp. 1135–1139, 2010.
- [6] C.-H. Chang and J. Ji, Eds., *Improved compressed sensing MRI with multi-channel data using reweighted l1 minimization*. IEEE, 2010.
- [7] T. T. Cai and Lie Wang, "Orthogonal matching pursuit for sparse signal recovery with noise," *Information Theory, IEEE Transactions on*, vol. 57, no. 7, pp. 4680–4688, 2011.
- [8] A. Bastounis and A. C. Hansen, "On the absence of the rip in real-world applications of compressed sensing and the rip in levels," *arXiv preprint arXiv:1411.4449*, 2014.
- [9] A. M. Tillmann and M. E. Pfetsch, "The computational complexity of the restricted isometry property, the nullspace property, and related concepts in compressed sensing," *Information Theory, IEEE Transactions on*, vol. 60, no. 2, pp. 1248–1259, 2014.
- [10] E. Candes and J. Romberg, "Sparsity and incoherence in compressive sampling," *Inverse problems*, vol. 23, no. 3, p. 969, 2007.